Methylene Blue-Containing Silica-Coated Magnetic Particles: A Potential Magnetic Carrier for Photodynamic Therapy

Dayane B. Tada,[†] Lucas L. R. Vono,[†] Evandro L. Duarte,[‡] Rosangela Itri,[‡] Pedro K. Kiyohara,[‡] Maurício S. Baptista,[†] and Liane M. Rossi*[,†]

Institute of Chemistry, University of São Paulo, São Paulo 05508-000, São Paulo, Brazil, and Institute of Physics, University of São Paulo, São Paulo 05508-090, São Paulo, Brazil

Received March 26, 2007. In Final Form: May 4, 2007

We present the preparation and characterization of methylene blue-containing silica-coated magnetic particles. The entrapment of methylene blue (MB), a photodynamic therapy drug under study in our group, in the silica matrix took place during the growth of a silica layer over a magnetic core composed of magnetite nanoparticles. The resulting material was charaterized by transmission electron microscopy (TEM), light scattering, and X-ray diffraction. It is composed of ∼30 nm silica spheres containing magnetic particles of 11 ± 2 nm and methylene blue entrapped in the silica matrix. The imobilized drug can generate singlet oxygen, which was detected by its characteristic phosphorescence decay curve in the near-infrared and by a chemical method using 1,3-diphenylisobenzofuran to trap singlet oxygen. The lifetime of singlet oxygen was determined to be 52 μs (in acetonitrile) and 3 μs (in water), with both values being in good agreement with those in the literature. The release of singlet oxygen (η_Δ) was affected by the encapsultation of MB in the silica matrix, which caused a reduction to 6% of the quantum yield of MB free in solution. The magnetization curve confirmed the superparamagnetic behavior with a reduced saturation magnetization in respect to uncoated magnetic nanoparticles, which is consistent with the presence of a diamagnetic component over the magnetite surface. The result is a single particle platform that combines therapy (photosensitizer) and diagnostic (MRI contrast agent) possibilities at the same time, as well as drug targeting.

Introduction

Magnetic carriers have been extensively applied in the fields of biotechnology and biomedicine for applications such as drug targeting,[1−4] cell sorting and isolation,[5−9] enzyme immobilization,[10−12] and magnetic resonance imaging.[13−15] The iron oxides are far the most used magnetic nanoparticles for biomedical applications, since they are much less toxic than their metallic counterparts, and they still have high saturation magnetization and superparamagnetic behavior, among which magnetite is a very promising choice due to its already proven biocompatibility.[16] Coprecipitation of Fe^{2+} and Fe^{3+} ions under alkaline conditions has been routinely used for the synthesis of magnetite nanoparticles,[17] although more elegant procedures involving high-temperature decomposition of iron(0) or iron(III) precursors stabilized by surfactant molecules have been reported.[18]

The biomedical applicability of magnetic nanoparticles is greatly improved by coating their surfaces with biocompatible organic polymers or inorganic metallic or oxide materials to protect the magnetic core and facilitate surface functionalization. Magnetic nanoparticles having suitable surface characteristics have a great potential for *in vitro* and *in vivo* applications.[19] In this work, we will explore the entrapment of methylene blue in a silica layer deposited over magnetic particle surfaces and the possible use of this new material as a magnetic drug carrier.

In particular, an increasing number of researchers have considered the possibility of using nanomaterials with drugs immobilized for photodynamic therapy (PDT).[20] Such a therapy is based on the concept that photosensitizer molecules generate reactive oxygen species upon irradiation, such as singlet oxygen ($^1O_2$) or free radicals, which can irreversibly damage the treated tissues.[21] In contrast to other conventional medical treatments, in PDT, it is unnecessary to release the loaded drug, and the

* To whom correspondence should be addressed. Telephone: +55 11 30912181. Fax: +55 11 38155579. E-mail: lrossi@iq.usp.br.
[†] Institute of Chemistry.
[‡] Institute of Physics.

(1) Pankhurst, Q. A.; Connolly, J.; Jones, S. K.; Dobson, J. *J. Phys. D: Appl. Phys.* **2003**, *36*, R167 and references therein.
(2) Lubbe, A. S.; Bergemann, C.; Riess, H. *Cancer Res.* **1996**, *56*, 4686.
(3) Gupta, P. K.; Hung, C. T. *Life Sci.* **1989**, *44*, 175.
(4) Fukushima, T.; Sekizaqa, K.; Jin, Y.; Yamaya, M.; Sasaki, H.; Takishima, T. *Am. J. Physiol.* **1993**, *265*, L67.
(5) Thomas, T. E.; Abraham, S. J. R.; Otter, A. J.; Blackmore, E. W.; Lansdorp, P. M. *J. Immunol. Methods* **1992**, *2*, 245.
(6) Sonti, S. V.; Bose, A. *J. Colloid Interface Sci.* **1995**, *170*, 575.
(7) Hancock, J. P.; Kemshead, J. T. *J. Immunol. Methods* **1993**, *164*, 51.
(8) Safarik, I.; Safarikova, M. *J. Chromatogr., B* **1999**, *722*, 33.
(9) Dyal, A.; Loos, K.; Noto, M.; Chang, S. W.; Spagnoli, C.; Sha, K. V. P. M.; Ulman, A.; Cowman, M.; Gross, R. A. *J. Am. Chem. Soc.* **2003**, *125*, 1684.
(10) Rossi, L. M.; Quach, A. D.; Rosenzweig, Z. *Anal. Bioanal. Chem.* **2004**, *380*, 606.
(11) Huang, S.-H.; Liao, M.-H.; Chen, D.-H. *Biotechnol. Prog.* **2003**, *19*, 1095.
(12) Chen, D.-H.; Liao, M.-H. *J. Mol. Catal. B: Enzym.* **2002**, *16*, 283.
(13) Cheng, F.-Y.; Su, C.-H.; Yang, Y.-S.; Yeh, C.-S.; Tsai, C.-Y.; Wu, C.-L.; Wu, M.-T.; Shieh, D.-B. *Biomaterials* **2005**, *26*, 729 and references therein.
(14) Taupitz, M.; Schnorr, J.; Abramjuk, C.; Wagner, S.; Pilgrimm, H.; Hunigen, H.; Hamm, B. *J. Magn. Reson. Imaging* **2000**, *12*, 905.
(15) Bades, L.; Denizot, B.; Tanguy, G.; Le Jeune, J. J.; Jallet, P. *J. Colloid Interface Sci.* **1999**, *212*, 474.
(16) Schwertmann, U.; Cornell, R. M. *Iron oxides in the laboratory: preparation and characterization*; VCH: Weinheim, 1991.
(17) For example: Vestal, C. R.; Zhang, G. J. *J. Am. Chem. Soc.* **2002**, *124*, 14312 and references therein.
(18) (a) Hyeon, T. *Chem. Commun.* **2003**, 927 and references therein. (b) Shen, S.; Zeng, H. *J. Am. Chem. Soc.* **2002**, *124*, 8204. (c) Sun, S.; Zeng, H.; Robinson, D. B.; Raoux, S.; Rice, P. M.; Wang, S. X.; Li, G. *J. Am. Chem. Soc.* **2004**, *126*, 273. (d) Woo, K.; Hong, J.; Choi, S.; Lee, H.-W.; Ahn, J.-P.; Kim, C. S.; Lee, S. W. *Chem. Mater.* **2004**, *16*, 2814.
(19) Gupta, A. K.; Gupta, M. *Biomaterials* **2005**, *26*, 3995.
(20) (a) Wang, S.; Gao, R.; Zhao, F.; Selke, M. *J. Mater. Chem.* **2004**, *14*, 487. (b) DeRosa, M. C.; Crutchley, R. J. *Coord. Chem. Rev.* **2002**, *233−234*, 351. (c) Zeitouni, N. C.; Oseroff, A. R.; Shieh, S. *Mol. Immunol.* **2003**, *39*, 1133. (d) Harrell, J. A.; Kopelman, R. *Biophotonics Int.* **2001**, *7*, 22. (e) Moreno, M. J.; Monson, E.; Reddy, R. G.; Rehemtulla, A.; Ross, B. D.; Philbert, M.; Schneider, R. J.; Kopelman, R. *Sens. Actuators, B* **2003**, *90*, 82. (f) Xu, H.; Buck, S. M.; Kopelman, R.; Philbert, M. A.; Brasuel, M.; Ross, B. D.; Rehemtulla, A. *Isr. J. Chem.* **2004**, *44*, 317. (g) Ross, B.; Rehemtulla, A.; Koo, Y.-E. L.; Reddy, R.; Kim, G.; Behrend, C.; Buck, S.; Schneider, R. J., II; Philbert, M. A.; Weissleder, R.; Kopelman, R. *SPIE−Int. Soc. Opt. Eng.* **2004**, *5331*, 76.
(21) Dougherty, T. J. *Photochem. Photobiol.* **1987**, *45*, 879.

10.1021/la700883y CCC: $37.00
Published on Web 06/23/2007

diffusion of surrounding oxygen molecules for the generation of active oxygen species is sufficient for therapeutic effects.[22] The encapsulation of PDT drugs in colloidal carriers such as micelles, liposomes, and polymer particles has been investigated.[23] Such drug carriers are preferentially taken up by tumor tissues due to the phenomenon known as the "enhanced permeability and retention effect", which is a property of tumor tissues to engulf and retain circulating macromolecules and particles. However, to provide selective drug delivery, it is still necessary to have a targeting approach based on surface modification with target tissue receptors or antigens. A nanoparticle approach for photosensitizer drug delivery based on gold nanoparticles whereby the photosensitizer is bound to the gold nanoparticle surface was reported.[24] Other nanoscale systems based on semiconductor quantum dots[25] and iron oxide nanoparticles[26] have also been published. In that study, the photosensitizer was covalently bound to naked iron oxide nanoparticle surfaces through a molecular anchor. A possible disadvantage of the approach based on the immobilization of drug molecules on the nanomaterial surfaces can be the reduced amount of loaded drug. Silica nanoparticles with the photosensitizer encapsulated within the nanoparticle matrix have been reported as highly loaded PDT drug carriers.[27−29] Silica is a very versatile material that can be prepared with a desired size, shape (nearly spherical particles), and porosity, and it is extremely stable. Because of the high stability, silica-based nanoparticles may not release any encapsulated drug even at extreme conditions of pH and temperature, but the porous matrix will be permeable to molecular as well as singlet oxygen. In addition, silica is known for its biocompatibility and ease of surface modification with a variety of functional groups using silane chemistry and commercially available organosilicon reagents for biotargeting.[30] Roy et al.[27] reported the encapsulation of 2-devinyl-2-(1-hexyloxyethyl) pyropheophorbide (HPPH), a water-insoluble photosensitizing anticancer drug, in 30 nm silica particles with good results. Yan et al.[29] reported the encapsulation of meta-tetra(3-hydroxyphenyl)-chlorin (m-THPC), a second-generation photosensitizer, in 180 nm silica spheres. Although the drug is embedded inside the particle matrix, it can be excited to efficiently generate singlet oxygen for photodynamic therapy.

Methylene blue (MB) is a photosensitizer with interesting photophysical and photochemical properties[31] that has shown impressive results in *in vivo* regression of cancer and microorganism infections.[32,33] There is a significant potential for clinical PDT applications of this low-toxicity photosensitizer when encapsulated in nanoparticles. Tang et al.[28] reported the encapsulation of MB in nanoparticles composed of polyacrylamide, sol−gel silica, and organically modified silicate (ORMOSIL). Each of these matrixes was characterized by diverse polymer properties and different degrees of MB loading. Among these, the sol−gel silica particles showed higher loading of MB. The generation of $^1O_2$ upon irradiation was shown by an indirect chemical method, and the delivery of $^1O_2$ was reduced to different extents by encapsulation. This difference in activity was attributed to the various microenvironments in the nanoparticles, in particular, the local sequestration of produced $^1O_2$ by the matrixes or even the dimerization of MB, which occurred in different extents in the matrixes. Among them, the sol−gel silica particles showed the best $^1O_2$ delivery capacity per milligram of particles.

The current work reports on the immobilization of methylene blue in a silica matrix, which conveniently coats magnetic particles, as a magnetic carrier for application in PDT. Magnetic localization of photosensitizer molecules can help to minimize the generation of cytotoxic substances in surrounding normal tissues. Also, the incorporated magnetic nanoparticles could be used as a magnetic resonance imaging (MRI) contrast agent to MRI tumor detection or in hyperthermia therapy. The result is a single particle platform that combines diagnostic and therapy possibilities at the same time.

Results and Discussion

Silica-coated magnetic particles containing methylene blue (MagMB) were prepared by modification of the procedure previously described by Philipse et al.[34] It consists of precoating the magnetic particle surfaces with soluble silicate and subsequent growth of a silica layer by condensation of tetraethylorthosilicate (TEOS) in the presence of the drug. The main problem in this kind of preparation is the stabilization of magnetic particles against aggregation before condensation of the silicon precursor TEOS. The precoating step proved to be necessary for the stabilization of the magnetic particles in an alcoholic solution used for the silica layer growth. Without this step, precipitation and agglomeration of the magnetic nanoparticles takes place immediately after the addition of ethanol or isopropanol. The magnetic cores were prepared by coprecipitation of Fe^{2+}/Fe^{3+} ions under alkaline conditions followed by stabilization with tetraethylammonium hydroxide. TEM images of the tetraethylammonium stabilized magnetic nanoparticles showed a size distribution from 5 to 17 nm in diameter (Figure 1). Analysis of the TEM micrographs revealed a monomodal particle size distribution with an average diameter of 11 ± 2 nm estimated by measuring the diameters of 200 randomly selected particles in enlarged TEM images. The histogram of Figure 1 shows the particle size distribution fitted by a Gaussian curve.

After the reaction with TEOS, a layer of silica was deposited on the iron oxide surfaces with MB molecules entrapped in the silica matrix. The deep blue solid was isolated by centrifugation and washed with ethanol until no more drugs could be detected in the supernatant by UV−vis spectroscopy. The particle size increased to ∼30 nm as can be seen from the TEM images shown in Figure 2. The morphology of the material is approximately spherical, but agglomeration can be seen. To better understand

(22) Snyder, J. W.; Skovsen, E.; Lambert, J. D. C.; Ogilby, P. R. *J. Am. Chem. Soc.* **2005**, *127*, 14558.

(23) (a) Konan, Y. N.; Gurny, R.; Allémann, E. *J. Photochem. Photobiol., B* **2002**, *66*, 89. (b) Roby, A.; Erdogan, S.; Torchilin, V. P. *Eur. J. Pharm. Biopharm.* **2006**, *62*, 235.

(24) (a) Hone, D. C.; Walker, P. I.; Evans-Gowing, R.; FitzGerald, S.; Beeby, A.; Chambrier, I.; Cook, M. J.; Russell, D. A. *Langmuir* **2002**, *18*, 2985. (b) Wieder, M. E.; Hone, D. C.; Cook, M. J.; Handsley, M. M.; Gavrilovic, J.; Russell, D. A. *Photochem. Photobiol. Sci.* **2006**, *5*, 727.

(25) (a) Samia, A. C. S.; Chen, X. B.; Burda, C. *J. Am. Chem. Soc.* **2003**, *125*, 15736. (b) Bakalova, R.; Ohba, H.; Zhelev, Z.; Nagase, T.; Jose, R.; Ishikawa, M.; Baba, Y. *Nano Lett.* **2004**, *4*, 1567.

(26) Gu, H.; Xu, K.; Yang, Z.; Chang, C. K.; Xu, B. *Chem. Commun.* **2005**, 4270.

(27) Roy, I.; Ohulchanskyy, T. Y.; Pudavar, H. E.; Bergey, E. J.; Oseroff, A. R.; Morgan, J.; Dougherty, T. J.; Prasad, P. N. *J. Am. Chem. Soc.* **2003**, *125*, 7860.

(28) Tang, W.; Xu, H.; Kopelman, R.; Philbert, M. A. *Photochem. Photobiol.* **2005**, *81*, 242.

(29) Yan, F.; Kopelman, R. *Photochem. Photobiol.* **2003**, *78*, 587−591.

(30) For example: (a) Rossi, L. M.; Shi, L.; Rosenzweig, Z. *Langmuir* **2005**, *21*, 4277. (b) Bagwe, R. P.; Zhao, X.; Tan, W. *J. Dispersion Sci. Technol.* **2003**, *24*, 453. (c) Badley, R. D.; Ford, W. T.; McEnroe, F. J.; Assink, R. A. *Langmuir* **1990**, *6*, 792.

(31) (a) Junqueira, H. C.; Severino, D.; Dias, L. G.; Gugliotti, M.; Baptista, M. S. *Phys. Chem. Chem. Phys.* **2002**, *4*, 2320. (b) Severino, D.; Junqueira, H. C.; Gabrielli, D. S.; Gugliotti, M.; Baptista, M. S. *Photochem. Photobiol.* **2003**, *77*, 459.

(32) Tardivo, J. P.; Del Giglio, A.; Oliveira, C. S.; Gabrielli, D. S.; Junqueira, H. C.; Tada, D. B.; Severino, D.; Turchiello, R.; Baptista, M. S. *Photodiag. Photodyn. Ther.* **2005**, *2/3*, 175.

(33) Tardivo, J. P.; Del Giglio, A.; Paschoal, L. H.; Baptista, M. S. *Photomed. Laser Surg.* **2006**, *24*, 528.

(34) Philipse, A. P.; van Bruggen, M. P. B.; Pathmamanoharan, C. *Langmuir* **1994**, *10*, 92.

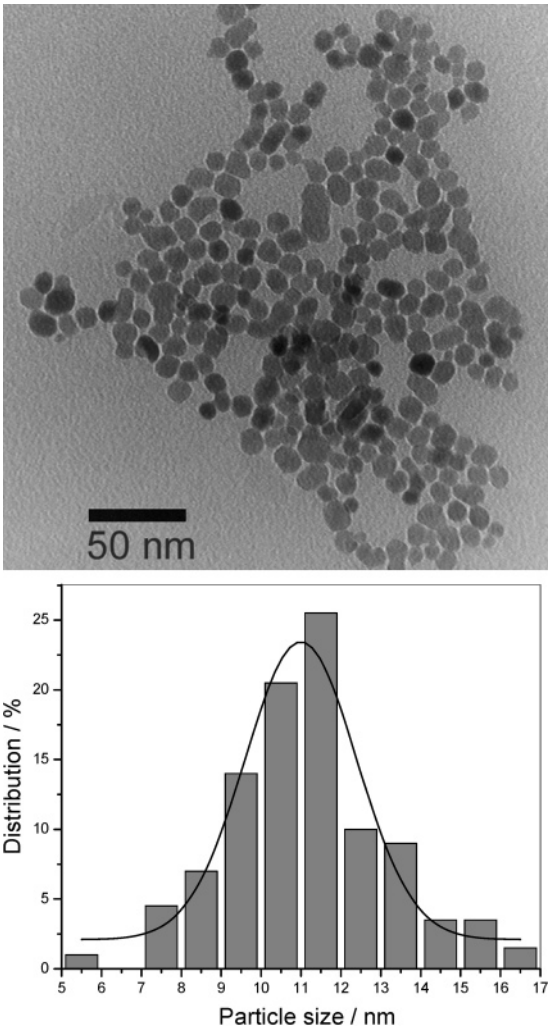

Figure 1. Transmission electron microscopy image of tetraethylammonium-stabilized magnetic nanoparticles (top) and particle size histogram showing a Gaussian size distribution fit (solid line) (bottom).

the behavior of a suspension containing the solid, we performed light scattering measurements and estimated the hydrodynamic diameter of the MagMB particles as 350 nm and the polydispersion as 0.18, which confirms the presence of aggregates in the suspension of particles.

The XRD patterns of the MagMB nanoparticles and the magnetic core are shown in Figure 3. The Bragg reflections present in both spectra at 30.06°, 35.42°, 43.00°, 53.38°, 56.90°, 62.56°, 71.06°, 74.04°, 79.10°, and 87.14° correspond to the indexed planes of cubic crystals of Fe_3O_4 (220), (311), (400), (422), (511), (440), (620), (533), (444), and (642). The iron oxide core average diameter for both samples could be estimated from the XRD diffraction pattern by means of the Debye−Scherrer equation calculated from full width at half-maximum (fwhm) of the most intense planes obtained from the Gaussian fit.[35] The magnetic core diameter calculated for both samples is 11 nm, which is consistent with that found by means of TEM images of uncoated magnetic nanoparticles (Figure 1). It means that the silica layer is not, indeed, crystalline, as indicated by the broad SiO_2 peak identified in the X-ray diffractogram (Figure 3b).

Concurrently, the magnetization curve displayed in Figure 4 revealed a superparamagnetic behavior of the MagMB nano-

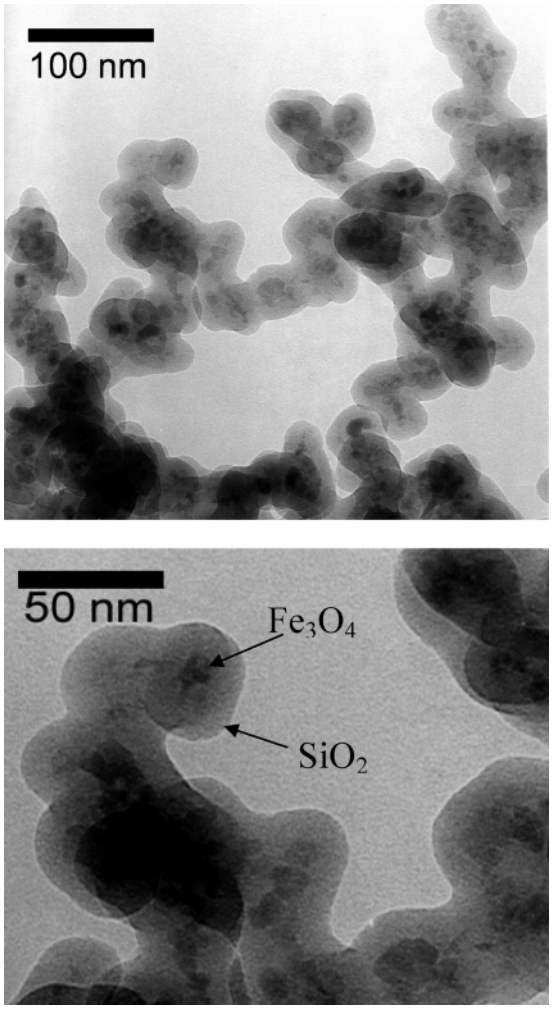

Figure 2. Transmission electron microscopy image of MagMB particles (top) and enlarged micrograph showing component details (bottom).

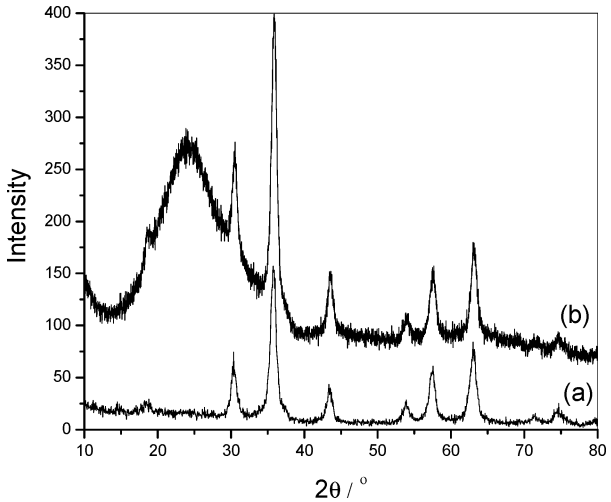

Figure 3. X-ray diffraction pattern of the (a) magnetic core−Fe_3O_4 nanoparticles and (b) MagMB particles.

particles with a saturation magnetization of 13 emu g^{-1}. This value is quite smaller than that observed for magnetite [92−100 emu g^{-1} (ref 36)], which is consistent with the presence of the diamagnetic component silicon dioxide. The observed decrease

(35) Cullity, B. D. *Elements of X-Ray Diffraction*; Addison-Wesley: Reading, MA, 1967.

(36) Cornell, R. M.; Schwertmann, U. *The Iron Oxides: Structure, Properties, Reactions, Occurrence and Uses*; VCH: Weinheim, 1996; p 117.

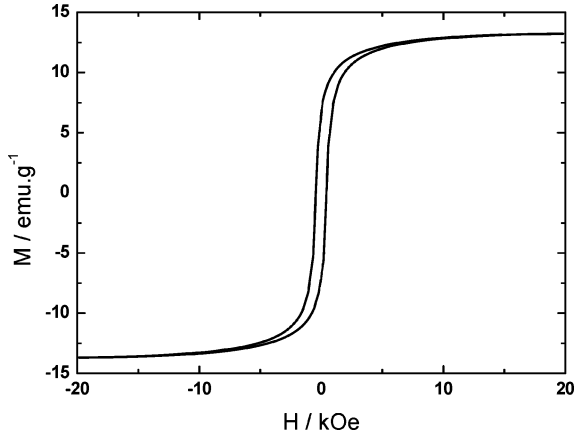

Figure 4. Magnetization curve of MagMB at 300 K.

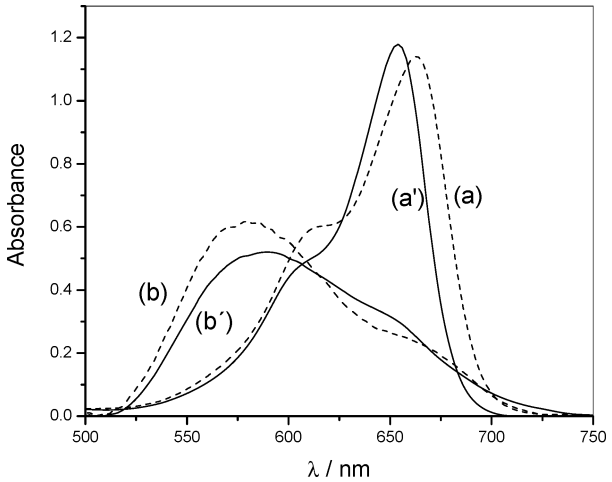

Figure 5. Absorption spectra of (a) an aqueous solution of MB free dye (15 μM), (b) an aqueous suspension of MagMB (1 mg mL^{-1}) (dashed lines), (a′) an acetonitrile solution of MB free dye (15 μM), and (b′) an acetonitrile suspension of MagMB (1 mg mL^{-1}) (solid lines).

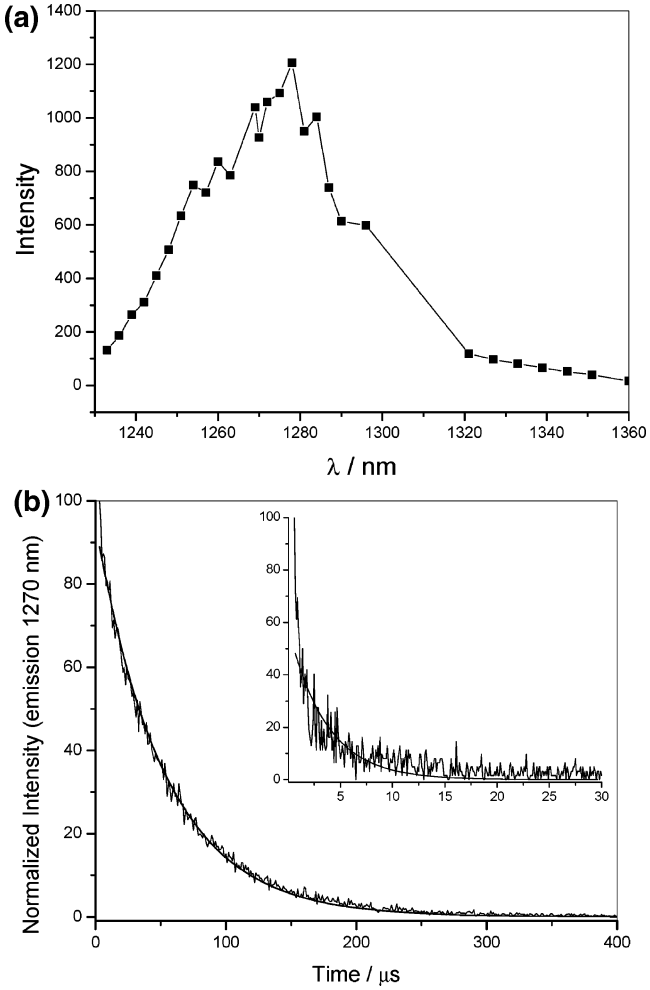

Figure 6. (a) Emission spectrum of singlet oxygen generated by MagMB particles in acetonitrile. (b) Emission transient at 1270 nm obtained after photoexcitation at 532 nm of MagMB particles in acetonitrile and aqueous solutions (inset).

of the saturation magnetization suggests the presence of ∼30% silica in the material.[37]

Regarding the photophysics and photochemistry properties of the MagMB, Figure 5 shows the absorption spectra of free MB and suspensions of MagMB particles in aqueous and acetonitrile solutions. The absorption spectrum of the MagMB suspension in both solvents is quite different from that observed for MB free in solution with λ_{max} = 664 nm (water) and λ_{max} = 654 nm (acetonitrile). A blue shift of the maximum absorption to 590 nm after immobilization in the silica matrix was observed, which can be attributed to aggregation and demethylation of MB molecules. The spectral fingerprint of MB aggregation is a blue shift that increases with aggregate size (dimer, trimers, and so forth). It can be seen that the shoulder at 600 nm observed in water decreased in acetonitrile solution, indicating a decrease in dimer concentration in this solvent. In the silica particles with MagMB, we probably have larger aggregates. The decrease in the 590 nm absorption band and the increase in the 650 nm shoulder in an acetonitrile suspension of MagMB indicate dislocation in the aggregate−monomer equilibrium. It also indicates that MB molecules entrapped in the silica matrix can be reached and affected by solvent molecules. Furthermore, the entrapment of MB is done in alkaline medium (pH 12) which can induce successive demethylation of MB in a time dependent process.[38] Therefore, the formed silica layer contains MB and some of its aggregates and demethylated products, mainly trimethyl thionine and asymmetric dimethyl thionine, which have similar quantum yields of singlet oxygen generation compared to MB.[31]

In this study, the detection of singlet oxygen was performed by a physical method based on the direct measurement of the near-infrared luminescence of $^1O_2$ at 1270 nm and by an indirect method using a chemical $^1O_2$ probe. The singlet oxygen generation was evidenced by the characteristic phosphorescence spectra obtained by monitoring the intensity of the phosphorescence at several wavelengths from 1260 to 1360 nm after photoexcitation of the MagMB suspensions, and the lifetime of singlet oxygen was determined from the phosphorescence decay curve at 1270 nm (Figure 6). The lifetime of singlet oxygen determined in acetonitrile solution was 52 μs, and in water it was 3 μs; both values are in good agreement with the values found in the literature for the lifetime of singlet oxygen in acetonitrile and aqueous solutions.[39] These results indicate that singlet oxygen, which is generated by the sensitizer immobilized in the silica matrix, diffuses through the solution. The singlet oxygen generation

(37) Haddad, P. S.; Duarte, E. L.; Baptista, M. S.; Goya, G. F.; Leite, C. A. P.; Itri, R. *Prog. Colloid. Polym. Sci.* **2004**, *128*, 232.

(38) Singhal, G. S.; Rabinowitch, E. *J. Phys. Chem.* **1967**, *71*, 3347.

(39) Wilkinson, F.; Helman, W. P.; Ross, A. B. *J. Phys. Chem. Ref. Data* **1993**, *24*, 663.

(40) Cao, Y.; Koo, Y-E. L.; Koo, S. M.; Kopelman, R. *Photochem. Photobiol.* **2005**, *81*, 1489.

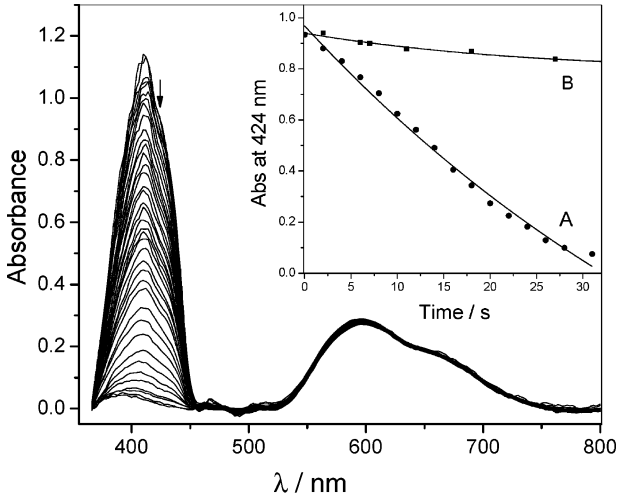

Figure 7. Absorption spectra of MagMB in the presence of DPBF after different times of irradiation with a 532 nm laser beam. Inset: Decay curves of absorption of DPBF as function of time of irradiation. (A) DPBF with MB free in solution and (B) DPBF with a dispersion of MagMB particles in acetonitrile.

efficiency (S_Δ) of a suspension of MagMB particles was estimated from eq 1 (see Experimental Section) to be 0.03 by measuring the phosphorescence emission intensity of $^1O_2$ at 1270 nm generated by MagMB in acetonitrile with a MB solution used as the standard.

The release of $^1O_2$ into the solution can be also estimated indirectly using 1,3-diphenylisobenzofuran (DPBF).[41] DPBF reacts irreversibly with $^1O_2$, which causes a decrease in the intensity of the DPBF absorption band at ~400 nm. By using two solutions with the same absorption at 532 nm (laser wavelength) and taking into account the scattering by the solid particles, we followed the decrease of the absorption intensity of DPBF with time upon irradiation in both solutions to estimate the efficiency of singlet oxygen release of the MagMB particles (Figure 7). Of note is the absence of a direct reaction of DPBF and MB once the MB absorption remains unchanged during the experiment. The singlet oxygen release (η_Δ) by a suspension of MagMB particles was estimated to be 0.03 ± 0.02, while the quantum yield of MB free in acetonitrile solution is ~0.5.[31] This value is in good aggreement with the singlet oxygen generation efficiency estimated by the physical method. This effect in the release of $^1O_2$ by encapsulted MB in nanoparticles has already been reported,[28] and it can be due to trivial effects, such as the scattering of the nanoparticles, the local sequestration of generated $^1O_2$ by the nanoparticle matrix, or an intrinsic lower encapsulated MB singlet oxygen quantum yield. We are presently working on the development of a spectroscopy setup for the measurement of absolute values of $^1O_2$ quantum yields (Φ_Δ) for nanoparticles.

Conclusions

We have prepared a nanoparticle-based drug carrier composed of a magnetic core and a silica layer containing the PDT drug methylene blue entrapped in the silica matrix. This approach, different from binding drugs directly to the magnetic particle surfaces, permits (i) increased loading of a positively charged drug, such as MB, in the negatively charged silica matrix; (ii) easy modification of drugs by reaction with organosilane reagents for entrapment in the silica matrix;[42] (iii) protection of the magnetic core against oxidation and agglomeration; and (iv) functionalization of the silica surface with different ligands for drug targeting to specific receptors. Although the drug is entrapped inside the silica matrix, it can be excited by irradiation to generate singlet oxygen that difuses into the solution, which can effect photodynamic therapy. *In vitro* experiments for nanoparticle uptake in cells and cell viability and *in vivo* evaluations of tumor regression are under investigation and will be the subject of a forthcoming report.

Experimental Section

Materials and Instrumentation. Iron(II) chloride hydrate, iron(III) chloride hydrate, methylene blue, and tetraethoxysilane were purchased from Sigma-Aldrich Chemical Co. Ammonium hydroxide 28−30% aqueous solution was purchased from J. T. Baker. All reagents and solvents were used as received without further purification. Deionized water used in the experiments was prepared to a specific resistivity of at least 18 MΩ cm.

Transmission electron microscopy (TEM) micrographs were taken on a Philips CM 200 microscope operating at an accelerating voltage of 200 kV. Samples for TEM observations were prepared by placing a drop containing the nanoparticles on a coated carbon grid. The metal particle size distribution was estimated from the measurements of ~200 particles, assuming a spherical shape, found in an arbitrary chosen area in the enlarged micrographs. X-ray diffraction (XRD) patterns were recorded on a Rigaku-Denki powder diffractometer equipped with a conventional X-ray generator (Cu Kα radiation λ = 1.5418 Å and graphite monochromator) coupled to a scintillation detector. The diffraction data were collected at room temperature with a scan range between 10° and 80°. A vibrating sample magnetometer (VSM) was used to obtain the magnetization versus magnetic field loop at room temperature up to H = 20 kOe. The apparatus was calibrated with a Ni pattern. The magnetization measurements were carried out on a known quantity of powder samples slightly pressed and conditioned in cylindrical holders of Lucite.

The generation of singlet oxygen and its lifetime were determined from phosphorescence decay curves at NIR. Data were recorded with a time-resolved NIR fluorimeter (Edinburgh Analytical Instruments) equipped with an Nd:YAG laser (Continum Surelite III) for sample excitation at 532 nm. The emitted light was passed through silicon and an interference filter and a monochromator before being detected at NIR-photomultiplier tube (Hamamatsu Co. R5509), according to a methodology reported elsewhere.[31] The singlet oxygen lifetime was determined by applying first-order exponential fitting to the curve of the phosphorescence decay at 1270 nm using Origin 7.0 software. The singlet oxygen generation efficiency (S_Δ) of MagMB particles was estimated from the relation given in eq 1, using a MB solution in acetonitrile as the standard.

$$S_{\Delta\text{particle}} = \phi_{\text{MB}} \frac{I_{\text{particle}}}{I_{\text{MB}}} \quad (1)$$

where I_{MB} is the phosphorescence emission intensity of $^1O_2$ at 1270 nm generated by MB free in acetonitrile solution, I_{particle} is the phosphorescence emission intensity of $^1O_2$ at 1270 nm generated by MagMB in acetonitrile, and ϕ_{MB} is the singlet oxygen quantum yield of MB free in acetonitrile solution given as 0.5.[31] The absorption of both solutions (MB and MagMB in acetonitrile) were normalized to the same values at 532 nm, assuming that we can calculate the real absorption of the photosensitizer immobilized in the particles by measuring the absorption spectrum of a suspension of MagMB and subtracting the baseline scattering by multiple point level baseline correction.

1,3-Diphenylisobenzofuran (DPBF), from Acros Organics, was used to determine the release of singlet oxygen into the solution by the particles at 16 °C in acetonitrile. The samples were immediately prepared before use by transferring 40 μL of DPBF stock solution (8 mM) to 2 mL of a suspension of MagMB or MB free solution,

(41) Spiller, W.; Kliesch, H.; Wohrele, D.; Hackbarth, S.; Roder, B.; Schnurpfeil, G. *J. Porphyrins Phthalocyanines* **1998**, *2*, 145.
(42) Collinson, M. M. *TrAC, Trends Anal. Chem.* **2002**, *21*, 30.

with the same absorption at 532 nm, in a quartz cuvette in the dark. The experiments were carried out by irradiating samples with a 532 nm laser beam provided by Morgotron, while absorption spectra were obtained after time intervals in a Shimadzu UV-2401PC spectrophotometer. The intensities of absorption at 424 nm were plotted against irradiation time, and the times for the decay of DPBF absorption were calculated by applying first-order exponential fitting to the curve obtained using Origin 7.0 software. The time for the decrease in absorption of DPBF (t) is inversely proportional to its reaction rate with singlet oxygen, and the inverse of time decay of absorption of DPBF caused by the photoexcitation of a suspension of particles in acetonitrile gives a measure of its singlet oxygen delivery ($\eta_{\Delta\text{particle}}$). A MB acetonitrile solution was used as the standard, and the relation given in eq 2 was used to calculate the release of singlet oxygen by the particles.

$$\eta_{\Delta\text{particle}} = \phi_{\text{MB}} \frac{t_{\text{MB}}}{t_{\text{particle}}} \quad (2)$$

where t_{MB} is the time for the decrease in absorption of DPBF in the presence of MB free in acetonitrile solution adjusted to a first-order exponetial decay, t_{particle} is the time for the decrease in absorption of DPBF in the presence of MagMB in acetonitrile adjusted to a first-order exponetial decay, and ϕ_{MB} is the singlet oxygen quantum yield of MB free in acetonitrile solution given as 0.5.[31]

Synthesis of Magnetic Particles. Fe_3O_4 nanoparticles were prepared by a coprecipitation method: 10 mL of an aqueous solution of $FeCl_3$ (1 mol L^{-1}) was mixed with 2.5 mL of $FeCl_2$ (2 mol L^{-1}) dissolved in 2 mol L^{-1} HCl. Both solutions were freshly prepared with deoxygenated water before use. Immediately after mixing under nitrogen, the solution containing the iron chlorides was added to 250 mL of ammonium hydroxide solution (0.7 mol L^{-1}, deoxygenated water) under vigorous mechanical stirring (10 000 rpm, Ultra-Turrax T18 Homogenizer, IKA Works) under nitrogen atmosphere. After 30 min, the black precipitate that formed was magnetically separated and then washed with water (3 × 250 mL). The obtained precipitate was dispersed in 110 mL of water and stabilized after addition of 15 mL of tetraethylammonium hydroxide. The final solution contained ~7 g L^{-1} Fe_3O_4 particles.

Synthesis of Methylene Blue-Containing Magnetic Silica Spheres. Silica-coated magnetic particles were prepared following the procedure described by Philipse et al.[34] A 0.58 wt % silicate solution (16 mL; the silicate solution was previously passed through an acid exchange resin column, and the pH was adjusted to 9.5 using a small portion of the original silicate solution) was mixed with 85 mL of ferrofluid stabilized with tetraethylammonium hydroxide (1.4 g L^{-1}). After mixing, the solution attained pH 12 and it was adjusted to pH 10 with 0.5 mol L^{-1} HCl. The solution was stirred for 2 h and then submitted to dialysis against an aqueous solution of tetraethylammonium hydroxide with the pH adjusted to 10 for 2 days. TEOS (0.08 mL) was added to a solution containing 75 mL of ethanol, 2.5 mg of methylene blue, 3.4 mL of NH_4OH, and 1 mL of the obtained particles (1.1 g L^{-1}). The solution was stirred for 24 h. The product was isolated by centrifugation (6000 rpm, 20 min) and then washed with ethanol until no more drug was detectable in the UV−vis spectra of the supernatant.

Acknowledgment. We are grateful to FAPESP, CNPq, and TWAS for financial support. We also thank the Magnetization Laboratory of IFUSP for VSM measurements.

LA700883Y